Crystalline inelastic response of high-density amorphous ice

M. M. Koza,[1] H. Schober,[1] B. Geil,[2] M. Lorenzen,[3] and H. Requardt[3]
[1]*Institut Laue-Langevin, F-38042 Grenoble Cedex, France*
[2]*Fachbereich Physik, Technische Universität Darmstadt, D-64289 Darmstadt, Germany*
[3]*European Synchrotron Radiation Facility, F-38042 Grenoble Cedex, France*
(Received 12 August 2003; published 30 January 2004)

Very high-resolution inelastic x-ray scattering is employed to determine the dynamic response of the high-density crystalline water phases ice IX and ice XII in the $Q=2.0$–15.5 nm^{-1} momentum transfer range. The spectra in the first and second Brillouin zone of the crystalline samples possess distinctive (Q,ω) dependencies. In particular, the response of ice IX gives evidence of the presence of an ensemble of excitations already at lowest Q. Similar features are found in the high-density amorphous water phase (HDA). The acoustic mode in HDA is well defined and little damped up to $Q=9$ nm^{-1}. Its slope is close to that of ice IX. Despite the apparent structural disorder of HDA its dynamic response appears crystal-like with a close resemblance to ice IX pointing at an intriguing high degree of short-range order.

DOI: 10.1103/PhysRevB.69.024204 PACS number(s): 63.50.+x, 64.70.Kb, 78.70.Ck

Amorphous polymorphism is known for almost 20 years when for the first time two different disordered solid states of water—a high-density amorphous (HDA) ($\rho\approx 39$ mol/nm^3) and a low-density amorphous (LDA) phase ($\rho\approx 31$ mol/nm^3)—were successfully prepared.[1] Since then tremendous efforts have been undertaken to give a coherent explanation for the existence of amorphous polymorphism. A wide span of different concepts have been proposed for HDA and LDA. One extreme identifies them as highly disordered crystalline states while the other extreme associates them with glassy forms of two distinct liquid phases, which are supposed to exist in the deeply super-cooled region of water's phase diagram.[2,3] To date the decisive evidence to distinguish the different concepts is still missing. Part of the problem resides in the fact that water's phase diagram places severe experimental limitations. Equally, experimental results obtained on amorphous ice modifications often do not show the characteristics typically associated with disordered systems.

One such characteristic feature of amorphous systems is the over damping of collective excitations with wavelength of the order of interparticle distances.[4,5] The topological disorder is expected to open up decay channels that appreciably reduce the phonon life time and thus lead to the extraordinary broadening observed by inelastic x-ray scattering (IXS). The well-known boson peak is supposed to constitute such a channel. Although the detailed interaction of collective modes with the boson peak is still an issue of debate[6,7] there is an emerging consensus upon the relation of these glassy features and the fragility of the system.[8] The stronger the glassy system the stronger seems the boson peak and the overdamping of its collective excitations.[4,9]

This coherent picture breaks down completely when LDA is taken into consideration where sharp excitations in complete accordance with those of cubic crystalline ice I_c (Ref. 10) are detected. This crystal-like behavior contrasts both with the liquid state and that of other glassy systems.[4,11,12] Moreover, it has been experimentally demonstrated that two level systems, which are another glass characteristic, are completely absent in LDA.[13] Thus, the association of LDA with a disordered crystal rather than a glass is tempting. In the case of HDA, the comparison with cubic crystalline ice is less convincing leaving the possibility of a connection with the inelastic response of the liquid.[11,12] However, it is well known that the diversity of water's crystalline phases is reflected in its dynamic characteristics.[14–16] For this reason, the interpretation of HDA's inelastic response may just necessitate the correct crystalline reference system.

In this paper we present inelastic x-ray data on two high-density polycrystals, namely ice IX ($P4_12_12$, $\rho\approx 39$ mol/nm^3) (Ref. 17) and ice XII ($I\bar{4}2d$, $\rho\approx 43$ mol/nm^3) in comparison to HDA. The equivalent preparation procedure of the crystalline phases and HDA (Ref. 18) and the close resemblance of their mass densities mark ice IX as well as ice XII *a priori* as suitable reference systems. Since the inelastic response of a sample is the spectral image of its force constant distribution the detailed properties of the response contain information on the potentials and thus of the H bonds in ice. As has been shown previously by extensively sampling the generalized density of states (GDOS) of solid water phases[14–16,19] the distortion of the H–bonded water network leaves specific fingerprints in the inelastic response, whereby the diversity of the H-bond angles in the different ice phases is reflected in an increasing complexity of their dynamics. Here, we go beyond the averaged spectral information contained in GDOS data and report on the properties of collective excitations, i.e., on the dispersion relation and linewidths of phonons. The inelastic responses of ice IX and ice XII do not only comprise valuable information towards the understanding of the HDA dynamics. They constitute highly interesting systems in themselves displaying strong differences in the H-bond response to density changes and H-bond angle distributions. As far as the correlation between the mass density and the H-bond angle distribution is concerned, ice XII is an outstanding system revealing the highest mass density of all ice phases without any ring interpenetration in the H-bond network.[18,20,21]

All studied samples are prepared by compressing hexagonal ice I_h in a piston-cylinder apparatus. HDA and ice XII are

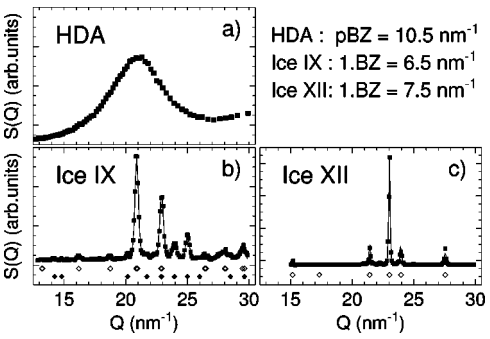

FIG. 1. The measured static structure factors of high-density amorphous ice (HDA), crystalline ice IX, and ice XII plotted as full rectangles in figures (a), (b), and (c), respectively. The crystalline structures are confirmed by Rietveld refinement indicated as full lines. In the sample we refer to as ice IX a contribution of at most ~16% of ice VI is found, details are given in the text. Bragg reflections are indicated by open diamonds for ice IX, full diamonds for ice VI in (b), and by open diamonds for ice XII in (c). The dimensions of the respective pseudo-Brillouin zone of HDA and the reduced 1st Brillouin zones of the crystalline structures are given in the upper right corner.

formed at a maximum pressure of 18 kbar at $T \approx 77$ K, ice IX is prepared at 10 kbar and $T = 150$ K.[18] During the compression the temperature T of the piston-cylinder apparatus is monitored and kept constant within 5 K of the nominal T. After the metastable samples have been cooled to $T \approx 77$ K and recovered from the pressure cells they are filled into cylindrical sample holders ($\varnothing = 15$ mm) with open windows and mounted therein onto a precooled displex ($T = 60$ K) used as sample environment.[10] The samples are measured on two IXS spectrometers at the European Synchrotron Radiation Facility (ESRF) in Grenoble, France. HDA is measured on ID16, the crystalline samples are studied on the equivalent spectrometer ID28. In both experiments the same sample environment and identical experimental conditions are applied. The initial x-ray energy is chosen to 21.7 keV ensuring a resolution of 1.6-meV full width at half maximum for inelastic scans.

X-ray photographs and elastic scans are used to verify a good powder average of the crystalline samples and the bulk amorphous state of HDA. Figure 1 shows the measured elastic intensities and results from Rietveld-refinement on the crystalline structures. A refinement under most stringent conditions confirms a contribution of at most 16% of ice VI to the sample prepared as ice IX. Only the amounts of ice IX, of ice VI, their cell parameters and the angular resolution of the spectrometer defined as Gaussian by a single parameter have been adjusted.[22] More sophisticated refining procedures result in an ice VI contribution even smaller than 10%. Within the accuracy of the refinement the presence of other ice phases can be excluded. The cell parameters obtained under the most stringent conditions are $a = 8.297(0.003)$ Å and $c = 4.031(0.003)$ Å for ice XII, $a = 6.71(0.01)$ Å and $c = 6.76(0.01)$ Å for ice IX, and $a = 6.237(0.004)$ Å and $c = 5.782(0.007)$ Å for ice VI. The content of ice VI is probably due to pressure gradients during the sample compression. Since, the inelastic signal depends linearly on the sample contents the amount of ice VI does not perturb significantly the interpretation of the inelastic response.

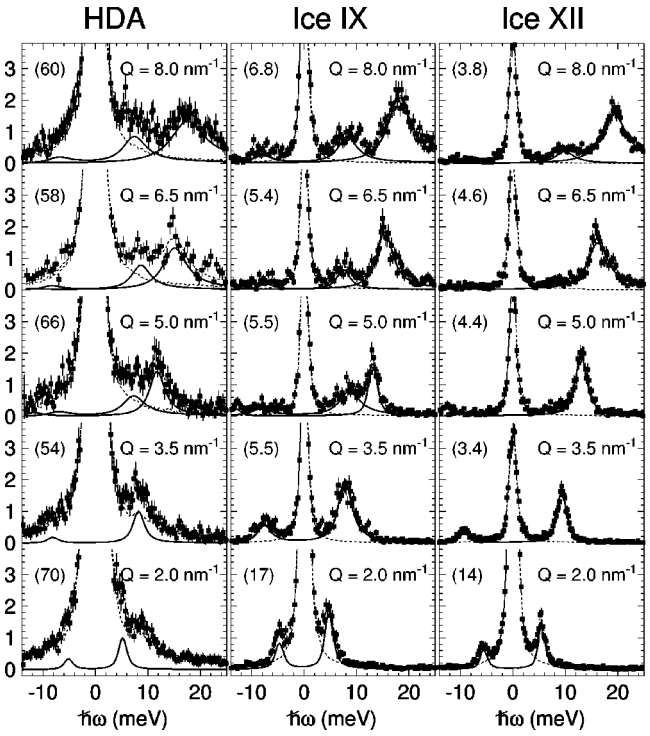

FIG. 2. IXS spectra of high-density amorphous (HDA), crystalline ice IX, and XII at the indicated Q values spanning the first Brillouin zone of the crystalline samples. The numbers on the left correspond to the elastic intensity. Dashed lines represent results from fits to the data as explained in the text. Full lines indicate the purely inelastic contribution.

The inelastic response is studied in constant Q mode in the range 2.0–15.5 nm^{-1}. Spectra up to $Q = 8$ nm^{-1} are shown in Fig. 2, three selected spectra at $Q > 8$ nm^{-1} are given in Fig. 3. For all spectra the maximum energy is chosen as 40 meV on the Stokes side covering entirely the range of phonon modes in the samples. In addition, the anti-Stokes side is measured down to ≈ -20 meV matching the range of acoustic excitations. To focus primarily on the inelastic re-

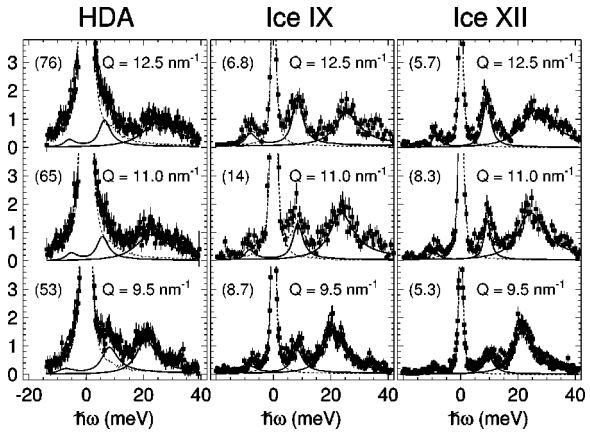

FIG. 3. Extension of the IXS spectra shown in Fig. 2 to Q-values exceeding the first Brillouin zone of ice IX and XII.

sponse the presented data are scaled arbitrarily. The elastic intensity is given in parentheses on the left-hand side of the elastic line in Figs. 2 and 3.

A comprehensive characterization of collective excitations in crystals necessitates the use of single crystalline samples, as the symmetry properties have to be fully exploited to determine the phonon eigenvectors and thus to discriminate, e.g., between acoustic and optic phonon branches, transverse and longitudinal polarization states. In practice, the phonon eigenvectors are determined in high-order Brillouin zones (BZ). Except for ordinary ice I_h (Refs. 11,12,15,23) no single-crystal material is available for other crystalline ice phases. The information on collective mode properties thus always envolves the averaging over all directions in reciprocal space. The effect of averaging is smallest for short wave vector transfers. To deduce the properties of collective excitations from powder samples the exploration of the entire 1st and the 2nd BZ's is mandatory, which is only achievable by high-resolution x-ray spectroscopy.[5] This does not only hold for polycrystalline samples like ice IX and XII but also for apparently disordered materials like HDA.

In the IXS technique, applied here, the interaction of photons with vibrational excitations in the sample is of purely coherent character.[5] For crystalline samples the dynamic structure factor $S(Q,\omega)$ depends thus on the selection rules of the phonons in the Q-space sampled by the experiment.[24] For example, purely transverse modes are not detectable within the 1st BZ. Thus, in cubic ice I_c only the longitudinal modes are observed as discussed in (Ref. 10). Structures of lower symmetry lead to complex phonon eigenvectors which contain both transverse and longitudinal components leading to complex and highly specific spectral shapes already in the 1st BZ.

The inelastic response of ice XII is governed by a rather sharp, dispersive maximum up to $Q=6.5\ \mathrm{nm}^{-1}$, i.e., throughout its reduced 1st BZ shown in Fig. 2. A second, nondispersive maximum around $\hbar\omega\approx 9.5$ meV is detected at Q-values exceeding the 1st BZ (Fig. 1). The energy range spanned by these modes corresponds to the regime of acoustic phonons.[19] We thus identify the maxima as the dispersive longitudinal acoustic phonon branch, and the non-dispersive transverse optic phonons which become detectable in the 2nd BZ. The well-defined onset of transverse modes at the boundary of the reduced 1st BZ gives evidence of the high symmetry of the ice XII structure. A behavior equally found in ices I_c and I_h[10–12] At higher Q shown in Fig. 3 both maxima cease to disperse. The transverse modes become strongly pronounced whereby the other maximum broadens progressively leading to an inelastic response reminiscent of the density of states of ice XII at highest Q values.[19]

The dynamic behavior of ice IX shows a remarkable broadening already deep within the reduced 1st BZ at $Q=3.5\ \mathrm{nm}^{-1}$. The dispersive maximum splits into two distinct maxima at $Q=5\ \mathrm{nm}^{-1}$ whereby the more intense maximum remains dispersive up to $Q=9.5\ \mathrm{nm}^{-1}$. At higher Q values it develops into a double peaked band with the peaks centred around 22 meV and 35 meV. In full accordance with transverse optic modes the second maximum emerging around 8 meV at $Q=5\ \mathrm{nm}^{-1}$ does not show any dispersive behavior, which proves the existence of modes with mixed polarization being detectable already at $Q=3.5\ \mathrm{nm}^{-1}$. This is indicated by the extraordinary width of the maximum in comparison to ice XII and I_c.[10]

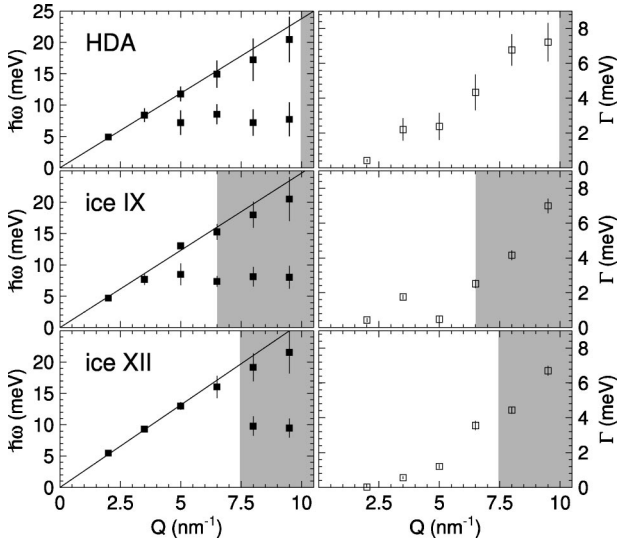

FIG. 4. Dispersion relation $\hbar\omega(Q)$ (left panel) of modes whose line shapes can be approximated by Lorentzian lines, and full width at half maximum (Γ) of the dispersive mode (right panel). Vertical lines through the data points indicate the respective Γ of the modes. The true error bars of $\hbar\omega(Q)$ would be of the order of the symbol size. Solid lines represent linear fits to the data up to 5 nm^{-1}. Please note the strong increase of the Γ at Q at which the nondispersive maximum becomes detectable, namely, at $Q=3.5\ \mathrm{nm}^{-1}$ (HDA, ice IX) and at $Q=6.5\ \mathrm{nm}^{-1}$ (ice XII). Gray shaded areas indicate the second pseudo-Brillouin zone of HDA and the second Brillouin zone of the crystalline samples, where in high-symmetry crystals and simple glasses transverse modes become detectable.

Despite the more intense elastic line the spectral shape of HDA resembles remarkably the response of ice IX, but not of ice XII. This is clearly stressed in Fig. 2 in the spectra taken at $5.0\ \mathrm{nm}^{-1}\leqslant Q\leqslant 8.0\ \mathrm{nm}^{-1}$. In complete equivalence to ice IX a dispersive peak can be well resolved from the elastic line in HDA. At $Q\geqslant 5.0\ \mathrm{nm}^{-1}$ a second, nondispersive maximum in between the elastic line and the dispersive mode can be unequivocally identified.

To quantify the observed features the spectra are fitted by a sum of Lorentzian functions convoluted with the experimentally determined resolution of the spectrometers and scaled by the detailed balance factor. In general three Lorentzians are used to account for the elastic line plus the dispersive and the nondispersive inelastic maxima.[25] For selected Q values a single Lorentzian is found sufficient to describe the inelastic signal.

The fit results are presented as lines in Figs. 2 and 3. The dispersion relation $\hbar\omega(Q)$ obtained from the fits is depicted in Fig. 4 for Q values at which the spectra can be reasonably approximated by one or two Lorentzians. Bars shown with the data points correspond to the full widths at half maximum (Γ) of the excitations. To stress the close resemblance of the phonon widths of all phases the Γ of the dispersive

maximum and their error bars are separately sketched in the right panel of Fig. 4. The gray shaded area is introduced to indicate the range of the pseudo-Brillouin zone for a disordered system[26] and the 2nd BZ of the crystalline samples, in which for high-symmetry crystals and simple glasses transverse modes are expected to become detectable.

A linear dependence of the phonon energy on Q can be reported up to $Q=5$ nm^{-1} in ice XII. In ice IX deviations from a linear dependence already at lower Q give evidence for a line shape that is more sophisticated than Lorentzian. This becomes particularly obvious at $Q=3.5$ nm^{-1}, where we equally observe a peak in the linewidth. A similar isolated enhancement of the linewidth is recorded in ice XII at $Q=6.5$ nm^{-1}, as well the very onset of the transverse mode signal. Strikingly, an unusually strong broadening of the line width is equally observed in HDA at exactly the same position as the one in ice IX. In the case of HDA it is difficult to observe this effect directly in the raw data as the strong elastic contribution tends to smooth out distinctive characteristics of the data as it has been recently elaborated in Ref. 6. Both, the order of magnitude and the detailed Q dependence of Γ are at pronounced variance from the properties of the liquid and of other glasses, where $\Gamma \sim Q^2$ or $\sim Q^4$ is expected.[4–7]

The translational invariance of crystalline structures implies that the dispersion of acoustic phonons should equally become evident in higher-order BZs. However, due to the spatial average in polycrystalline samples the number of Bzs sampled increases strongly with increasing Q leading to a smearing of the measured signal. With the additional strong contribution from the low energy optic modes an unequivocal quantification of dispersion properties beyond the 1st BZ of the polycrystalline samples is not possible, although, variations of the maxima below 10 meV contingent on Q are observed.

The velocity of sound is determined via the relation $v \sim \hbar\omega/Q$ as $v_{\mathrm{HDA}}=3640\pm70$ m/s, $v_{\mathrm{IX}}=3660\pm130$ m/s and $v_{\mathrm{XII}}=4060\pm50$ m/s. The error is estimated by taking different data intervals up to $Q=5.0$ nm^{-1} into consideration as it is indicated in Fig. 4. In this work, v_{HDA} tends towards a slightly higher value than the one reported in (Ref. 10) The deviation is due to changes in the data analysis: motivated by the similarity with the spectra of ice IX, here, the HDA data are decomposed with a higher number of Lorentzian lines at $Q \geqslant 5.0$ Å. Despite the elevated uncertainties $v_{\mathrm{IX}} \approx v_{\mathrm{HDA}}$. In particular in the case of the non-cubic ice IX and HDA the calculated velocities do not reflect the characteristics of a single propagating phonon branch. They have to be understood as a weighted average of group velocities obtained over all directions in reciprocal space. As the weighing is specific to the experimental probe care has to be taken when comparing with results obtained by some different technique.[28] Despite this fact, it should be noted that for ice III[17] $v_{\mathrm{III}}=3700$ m/s ($\pm1.5\%$) from Brillouin-scattering[29] and for HDA $v_{\mathrm{HDA}}=3700\pm50$ m/s from ultrasonic measurements[30] are reported and compare well with the values found in this paper.

In conclusion, we show by IXS that high-density crystalline ice IX and ice XII possess a distinguishable dynamic response throughout the sampled Q space. The most distinctive finger prints are observed within the reduced 1st BZ. Ice XII reveals up to $Q=5$ nm^{-1} a well-defined, single excitation, namely, the longitudinal acoustic phonon. Only above $Q \approx 6.5$ nm^{-1} a second nondispersive maximum, comprising transverse optic modes, is detectable. In complete contrast, the inelastic response of ice IX has a sophisticated spectral shape already at lowest Q values. Although, the spectra can be approximated by two broad excitation bands one of which showing a dispersive behavior, this dispersive mode cannot be characterized as a pure longitudinal phonon but as an ensemble of modes. In full accordance with the present IXS data a higher complexity of the spectral properties of ice IX in comparison to ice XII can be deduced from inelastic neutron and Raman scattering experiments.[15,19,31,32]

The ice IX spectral characteristics are equally encountered in the high-density amorphous ice phase. Moreover, specific quantities like the velocity of sound and the energy of the nondispersive, optic modes are identical in ice IX and HDA.

The results stress clearly that despite the apparent structural disorder displayed by $S(Q)$ in Fig. 1 the inelastic properties of HDA are those of a crystal with strong resemblance to ice IX. These properties are unequivocally distinguishable from the dynamics of the phases ice XII, ice I_c and LDA. It is of great importance to notice that the difference between HDA and LDA cannot be explained by the difference in density of these states. As it has been shown recently in pressure dependent IXS experiments[33] density changes up to 25% in liquid water are not able to change its spectral shape significantly. Consequently, the dynamic distinctness of HDA and LDA is just another manifestation of their exclusive character: They are distinct from each other and they are distinct from the liquid state.

In the general context of amorphous systems HDA violates apparently the concept of a quasi-Brillouin zone, as defined via Q_{quasi}, half the distance to the static structure factor maximum.[26] It is generally assumed and has recently been shown[34] that in simple glasses the response below Q_{quasi} is dominated by the longitudinal acoustic branches. This concept holds in LDA with $Q_{\mathrm{quasi}}^{\mathrm{LDA}}=8.5$ nm^{-1}.[10] However, in HDA despite $Q_{\mathrm{quasi}}^{\mathrm{HDA}}=11$ nm^{-1} the onset of a nondispersive mode is observed already at 3.5–5.0 nm^{-1}. Recent molecular dynamics simulations on a Lennard–Jones glass indicate that this implies a high degree of short-range order.[27] On the one hand, results obtained for the Lennard–Jones glass explain the dynamic properties reported in (Ref. 34) and thus support the concept of a quasi-Brillouin zone.[26] On the other hand, the results evaluated for the icosahedrally highly short-range ordered system match perfectly the dynamic response observed in HDA. The data presented in this paper give evidence that the type of short-range order in HDA is comparable to the one of ice IX. As a consequence, the strong maximum in $S(Q)$ in HDA does not characterize the maximum correlation length in the same way as the strongest Bragg reflections do not characterize the largest lattice spacings in ice IX and XII (Fig. 1).

Finally the presence of a high degree of short-range order can explain why a boson peak is suppressed in both amor-

phous structures.[16,35] A classification of HDA and LDA in terms of fragility, boson peak intensity and overdamping of acoustic excitations, as it has been successfully done for glassy systems,[4,9] is obviously not applicable to LDA and HDA. The inelastic response of both amorphous states meets the condition for a new class of amorphous materials.[36]

We acknowledge M. Krisch and A. Mermet for help and instructive discussions.

[1] O. Mishima, L.D. Calvert, and E. Whalley, Nature (London) **310**, 393 (1984).
[2] G.P. Johari, Phys. Chem. Chem. Phys. **2**, 1567 (2000).
[3] O. Mishima and H.E. Stanley, Nature (London) **396**, 329 (1998).
[4] F. Sette, M.H. Krisch, C. Masciovecchio, G. Ruocco, and G. Monaco, Science **280**, 1550 (1998).
[5] G. Ruocco and F. Sette, J. Phys.: Condens. Matter **13**, 9141 (2001).
[6] M. Foret, R. Vacher, E. Courtens, and G. Monaco, Phys. Rev. B **66**, 024204 (2002).
[7] B. Ruffle, M. Foret, E. Courtens, R. Vacher, and G. Monaco, Phys. Rev. Lett. **90**, 095502 (2003).
[8] C.A. Angell and W. Sichina, Ann. N.Y. Acad. Sci. **279**, 53 (1976).
[9] A.P. Sokolov, R. Calemczuk, B. Salce, A. Kisliuk, D. Quitmann, and E. Duval, Phys. Rev. Lett. **78**, 2405 (1997).
[10] H. Schober, M.M. Koza, A. Tölle, C. Masciovecchio, F. Sette, and F. Fujara, Phys. Rev. Lett. **85**, 4100 (2000).
[11] F. Sette, G. Ruocco, M. Krisch, C. Masciovecchio, R. Verbeni, and U. Bergmann, Phys. Rev. Lett. **77**, 83 (1996).
[12] G. Ruocco, F. Sette, M. Krisch, U. Bergmann, C. Masciovecchio, and R. Verbeni, Phys. Rev. B **54**, 14 892 (1996).
[13] N.I. Agladze and A.J. Sievers, Phys. Rev. Lett. **80**, 4209 (1998); N.I. Agladze and A.J. Sievers, Europhys. Lett. **53**, 40 (2001).
[14] D.D. Klug, E. Whalley, E.C. Svensson, J.H. Root, and V.F. Sears, Phys. Rev. B **44**, 841 (1991).
[15] Jichen Li, J. Chem. Phys. **105**, 6733 (1996).
[16] H. Schober, M. Koza, A. Tölle, F. Fujara, C.A. Angell, and R. Böhmer, Physica B **241–243**, 897 (1998).
[17] The present experiment is not able to discriminate between ice III and ice IX whose difference is determined only by the degree of disorder in the proton sublattice.
[18] M.M. Koza, H. Schober, T. Hansen, A. Tölle, and F. Fujara, Phys. Rev. Lett. **84**, 4112 (2000).
[19] M. Koza, H. Schober, A. Tölle, F. Fujara, and T. Hansen, Nature (London) **397**, 660 (1999).
[20] C. Lobban, J.L. Finney, and W.F. Kuhs, Nature (London) **391**, 268 (1998).
[21] M. O'Keeffe, Nature (London) **392**, 879 (1998).
[22] Partial atomic coordinates are taken from ice IX: S.J. LaPlaca, W.C. Hamilton, B. Kamb, and A. Prakash, J. Chem. Phys. **58**, 567 (1973); ice VI: W.F. Kuhs, J.L. Finney, C. Vettier, and D.V. Bliss, *ibid.* **81**, 3612 (1984); ice XII: (Ref. 18).
[23] B. Renker, in *Physics and Chemistry of Ice*, edited by E. Whalley, S.J. Jones, and L.W. Gold, (University of Toronto Press, Toronto, 1973), p. 82.
[24] J.M. Perez-Mato, M. Aroyo, J. Hlinka, M. Quilichini, and R. Currat, Phys. Rev. Lett. **81**, 2462 (1998).
[25] Other model functions like a damped-harmonic oscillator (Refs. 4 and 5) result in fits of poorer quality (Ref. 10).
[26] G.S. Grest, S.R. Nagel, and A. Rahman, Phys. Rev. Lett. **49**, 1271 (1982); G.S. Grest, S.R. Nagel, and A. Rahman, Phys. Rev. B **29**, 5968 (1984).
[27] S.I. Simdyankin, M. Dzugutov, S.N. Taraskin, and S.R. Elliott, Phys. Rev. B **63**, 184301 (2001).
[28] O. Andersson and H. Suga, Phys. Rev. B **65**, 140201(R) (2002).
[29] R.E. Gagnon, H. Kiefte, M.J. Clouter, and E. Whalley, J. Chem. Phys. **92**, 1909 (1990).
[30] E.L. Gromnitskaya, O.V. Stal'gorova, V.V. Brazhkin, and A.G. Lyapin, Phys. Rev. B **64**, 094205 (2001).
[31] J.E. Bertie, and B.F. Francis, J. Chem. Phys. **72**, 2213 (1980); **77**, 1 (1982).
[32] C. Salzmann, I. Kohl, T. Loerting, E. Mayer, and A. Hallbrucker, J. Phys. Chem. B **106**, 1 (2002).
[33] M. Krisch, P. Loubeyre, G. Ruocco, F. Sette, A. Cunsolo, M. D'Astuto, R. LeToullec, M. Lorenzen, A. Mermet, G. Monaco, and R. Verbeni, Phys. Rev. Lett. **89**, 125502 (2002).
[34] T. Scopigno, E. Pontecorov, R. Di Leonardo, M. Krisch, G. Monaco, G. Ruocco, B. Buzicka, and F. Sette, J. Phys.: Condens. Matter **15**, 1269 (2003).
[35] C.A. Tulk, D.D. Klug, E.C. Svensson, V.F. Sears, and J. Katsuras, Appl. Phys. A: Solids Surf. **74**, 1185 (2002).
[36] C.A. Angell, C.T. Moyniham, and M. Hemmati, J. Non-Cryst. Solids **274**, 319 (2000).